JOURNAL OF PROPULSION AND POWER
Vol. 21, No. 1, January–February 2005

Spray Detonation Initiation by Controlled Triggering of Electric Dischargers

S. M. Frolov* and V. Ya. Basevich†
N. N. Semenov Institute of Chemical Physics, 119991, Moscow, Russia
and
V. S. Aksenov‡ and Polikhov S. A.§
Moscow Physical Engineering Institute, 115522, Moscow, Russia

Experimental studies of single-pulse and multipulse confined detonations of liquid *n*-hexane spray in air initiated by successively triggered electric dischargers are presented. Similarly to a single-pulse mode, the multipulse operation mode shows the resonant dependence of the detonation initiation energy on the time delay between triggering the dischargers. There is a potential for considerable decrease in the detonation initiation energy with decreasing tube diameter and mounting of a turbulizing spiral between the dischargers. The technique is considered promising for pulse-detonation engine applications.

Nomenclature

C_1, C_2	=	capacitances of the main discharge of the dischargers D_1 and D_2
E	=	discharge energy
E_{cr}	=	critical energy of detonation initiation
E_p	=	energy of the primary (initiating) discharge
J_1, J_2	=	discharge currents for the dischargers D_1 and D_2
t_1, t_2, t_3	=	shock wave arrival times at pressure transducers PT1, PT2, and PT3, respectively
U	=	discharge voltage
U_i	=	voltage at which the dischargers D_1 and D_2 are triggered
U_T	=	threshold voltage
V	=	mean shock wave velocity
V_1, V_2, V_3	=	mean shock wave velocities at the measuring segments 1, 2, and 3
X	=	measuring segment length
ΔE	=	uncertainty in the discharge energy
Δt	=	uncertainty in measuring the time interval
Δt_d	=	time delay for triggering the discharger D_2
ΔU	=	uncertainty in the discharge voltage
$\Delta\tau_1$, $\Delta\tau_2$	=	intrinsic time delays of the dischargers D_1 and D_2

I. Introduction

ENERGY requirements for direct detonation initiation in liquid hydrocarbon fuel–air mixtures are very stringent.[1–4] Moreover, considerable fuel vapor content in a two-phase system is required for detonation initiation.[3] Therefore, to obtain detonations in a pulse-detonation engine (PDE), various means of promotion have to be combined, including reactive mixture preconditioning,[5–7] formation of a stratified mixture composition in the vicinity of initiators,[8–10] and cumulation of blast waves.[11–13] Use of distributed external energy sources to artificially accelerate an initially weak, propagating shock wave to a detonation by stimulating strong coupling between the shock wave and chemical-energy deposition is also one of the promising means of decreasing the initiation energy and shortening the predetonation distance.[14–19]

The objective of the research summarized in this paper is to further evaluate and experimentally realize one concept of a liquid-fueled air-breathing PDE, the shock-booster concept.[14–19] The results discussed herein were partly published in Ref. 20.

The idea of the shock-booster PDE is to repeatedly initiate a weak shock wave and to accelerate it by in-phase triggering of distributed electric dischargers in the course of shock wave propagation along a detonation tube. The use of external ignition sources to initiate a detonation was first suggested by Zel'dovich and Kompaneetz.[21] Later, this issue was studied computationally[15,22,23] and reviewed elsewhere.[24–26] For gaseous fuel (propane), detonation initiation by distributed external ignition sources has been demonstrated experimentally.[14–16] To substantiate this concept for liquid fuel sprays, several experimental facilities were designed, fabricated, and used during previous research.[17–19] Liquid *n*-hexane and *n*-heptane spray detonation was initiated in a single-pulse mode by one electric discharger or by two and three successively triggered dischargers in a tube with a flow of air and fine fuel drops produced by an air-assist atomizer. The effect of discharge time, shape, and location, tube insulating properties, shape and diameter, atomizer performance, distance between dischargers, and time delay between their triggering was studied.

Sections I and II of the present paper describe a new experimental facility and studies aimed at obtaining multipulse detonations with two successively triggered electric dischargers. Section III deals with optimization studies to demonstrate the possibility of obtaining the detonation initiation energy, tube length, and performance stability feasible for PDE applications.

II. Two-Discharge Multipulse Experimental Facility

A. Experimental Setup

A schematic of the experimental setup is shown in Fig. 1. The detonation tube comprises an air-assist atomizer and two sections: a booster section and a measuring section. The tube diameter is 51 mm. The air receiver of volume 40 liters is supplied with compressed air by a compressor. Air is fed to the atomizer via valve 1. Liquid fuel is fed to the atomizer from a pressurized fuel tank via valve 2. Both air and fuel supply can be either continuous or intermittent. The fuel used in all the experiments reported herein is liquid *n*-hexane. The booster section contains two dischargers (D_1 and D_2) mounted between the atomizer and the measuring section. Discharger D_1 is located at a distance of 60 mm downstream from the atomizer nozzle. The distance between D_1 and D_2 is 200 mm.

Received 21 October 2003; revision received 2 July 2004; accepted for publication 2 July 2004.

*Director of Laboratory, Department of Combustion and Explosion, 4, Kosigin Street; smfrol@center.chph.ras.ru.
†Chief Scientist, Department of Kinetics and Catalysis, 4, Kosigin Street.
‡Engineer, Department of Technical Physics, 31, Kashirskoe Shosse.
§Postgraduate Student, Department of Technical Physics, 31, Kashirskoe Shosse.

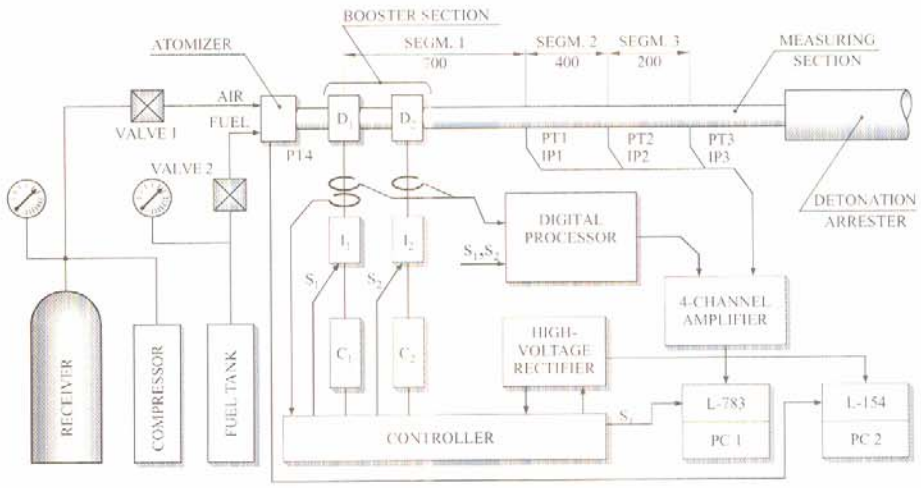

Fig. 1 Schematic of the experimental setup. Dimensions in millimeters.

The measuring section is 1 m long. It is equipped with three piezoelectric pressure transducers (PT1, PT2, and PT3) and three ionization probes (IP1, IP2, and IP3) mounted in the same cross sections. The pressure transducers and ionization probes form two measuring segments 400 and 200 mm long, respectively (SEGM. 2 and 3 in Fig. 1). Measuring segment 1 (SEGM. 1) is set from the center of the discharger D_1 to the position of PT1/IP1 and is 700 mm long. The measuring section is connected to the atmosphere through a detonation arrester.

A high-voltage rectifier with a maximal voltage of 3.5 kV and remote control is used to feed the discharger circuits. The rectifier provides the operating voltage to charge the capacitors C_1 and C_2 via a distributor (not shown in Fig. 1) and a digital controller. The controller, based on a preset program, activates the units I_1 and I_2, which, in their turn, activate dischargers D_1 and D_2, respectively. The energy deposition by the electric dischargers results in ignition of the fuel spray and generation of shock and detonation waves in the facility.

The data acquisition system is composed of two subsystems, allowing registration of processes over two essentially different time scales. A two-channel subsystem (L-Card L-154) with a sampling time interval of 5 ms registers the voltage at the capacitors and the air pressure in the atomizer (with pressure transducer PT4). A four-channel subsystem (L-Card L-783) registers up to 3000 samples per channel with an interval of 300×4 ns. The first three channels register the signals of the pressure transducers PT1, PT2, and PT3. The fourth (control) channel is used either for recording the combined signal of the ionization probes IP1, IP2, and IP3 or for the diagnostics of discharge timing. The maximum power provided by the rectifier is 1300 W. A power level exceeding 90% of the maximum power is attained at voltages between 1250 and 2250 V.

The velocity of the combustion fronts, as well as of the shock and detonation waves, was calculated using the formula $V = X/\Delta t$, where X is the length of the measuring segment and Δt is the time interval determined from the records of the ionization probes and/or pressure transducers. The systematic error in determining X is ± 0.5 mm; the accidental error is zero. At the third measuring segment, which is 200 mm long, this results in an error of $\pm 0.25\%$. The time interval Δt is determined at the half-amplitude levels of the ionization-probe or pressure-transducer signals. Because of the finite dimensions of the sensitive elements of the probes and transducers (8 mm), the duration of the shock and detonation front registration is no less than 3 μs. The characteristic sampling time of each measuring channel is 1.2 μs, which allows the resolution of the wave front with two to three samples. Thus the uncertainty in determining the arrival time at the position of the sensitive element did not exceed ± 1.2 μs, and therefore the time interval Δt was determined with an uncertainty of ± 2.4 μs. The detonation velocity in the n-hexane–air mixture is at the level of 1700–1800 m/s. The mean time interval taken for the detonation wave to pass the third measuring segment, which is 200 mm long, is about 115 μs. Hence the maximal error in determining the time interval Δt is $\pm 2\%$ at the third measuring segment and $\pm 1\%$ at the second measuring segment, and the error in determining the detonation velocity at these measuring segments does not exceed 2.25% and 1.25%, respectively. The shock-wave velocities in the experiments are smaller than the detonation velocity. Therefore the error of determining the shock-wave velocity is smaller than that for the detonation velocity.

B. Controller

The controller consists of several units that implement the preset algorithm of facility operation and provide operational safety. A remote control unit allows the triggering of a timer from a control room. The timer sets up the operation time of the facility, either for a preset limited period (from 0.5 to 10 s) or for unlimited operation. The timer sets up time limitations for the operation of three power relays controlling the air and fuel valves and the high-voltage rectifier. The rectifier is activated for the whole duration of an experimental run; however, it can be switched off automatically by a blocking system in case of a failure of the dischargers or by a command of the controller according to the operation algorithm.

Figure 2 illustrates the controller operation. Here, the supply of air and fuel (see the middle plot) is activated when the capacitor voltage attains a preset threshold value U_T (see the upper plot). At the time when the voltage increases to the U_i level, the controller generates the synchronizing pulses S_1 and S_2 (see the lower plot and extension), which activate the dischargers D_1 and D_2 as well as cutting air and fuel supply (see the middle plot). As a result, the voltage at the capacitors drops down. After decay of the discharge currents, the next operation cycle starts. Due to a special distributor unit the capacitors of the dischargers D_1 and D_2 are charged to the same voltage and discharged independently from each other according to a prescribed time schedule. The extension in Fig. 2 shows two synchronizing pulses, S_1 and S_2, and the records of currents J_1 and J_2 for the dischargers D_1 and D_2. The discharge currents occur with time delays $\Delta\tau_1$ and $\Delta\tau_2$ after the corresponding synchronizing pulses. These delays are the stochastic variables depending on the discharger design and voltage. The controller provides the time delay Δt_d for triggering the second discharger D_2. The time delay Δt_d is set from the origin of current J_1 to eliminate the effect of the

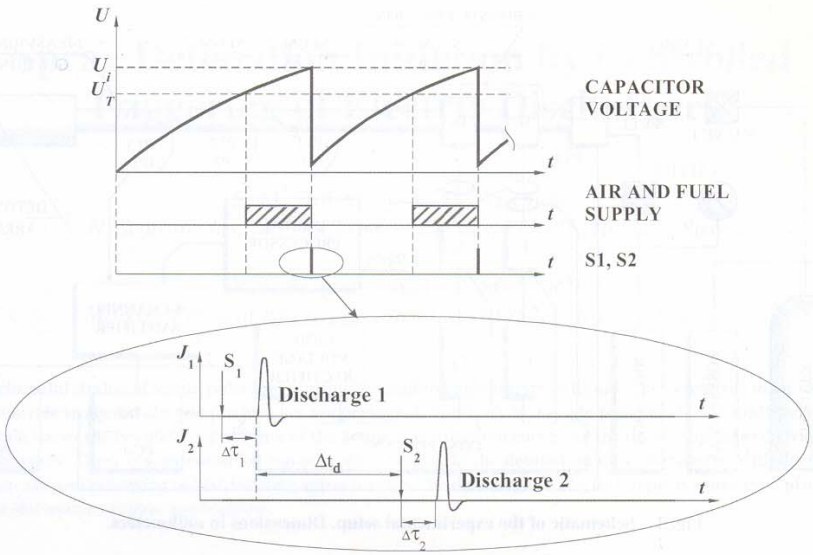

Fig. 2 Diagram illustrating controller operation.

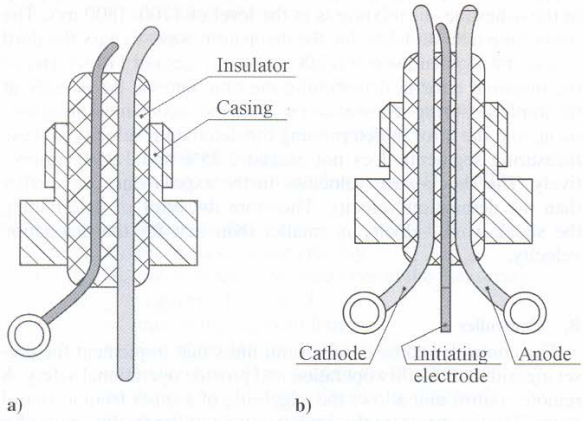

Fig. 3 Schematic of the discharger: a) side view, b) front view.

accidental time delays $\Delta\tau_1$ and $\Delta\tau_2$ and to improve the repeatability of the detonation initiation cycles.

C. Dischargers

The optimal design of the dischargers used in the facility was found by testing several tens of configurations.[17–19] The schematic of the discharger with three electrodes is shown in Fig. 3. Two power electrodes, the anode and cathode, are made of copper wire 4 mm in diameter. They protrude from the tube wall by 14 mm and are bent a little along the flow direction. The initiating electrode is made of copper wire 3 mm in diameter and is positioned upstream from the power electrodes. The gap between the initiating electrode and the cathode is 2 mm at the tip. The distance between the cathode and anode at their tips is 16 mm. The casing of the discharger is made of steel and has a thread to be fixed in the port of the detonation chamber. A cylindrical insulator 20 mm in diameter is made from Teflon and is fixed in the casing with a composite containing glass fiber and epoxy compound. The electric connections are made of a copper wire of cross section 2×2.5 mm and length 300 mm. The plasma cloud of the initiating discharge (current about 100 A) reaches the anode 20 μs after triggering the initiating pulse. The electric scheme of the discharger is conventional and provides a current pulse of duration 25 μs.

The initiating (primary) discharge is of fixed energy ($E_p = 57$ J). It produces plasma to trigger a main (power) discharge of considerably higher energy. The capacitance of the main discharge, C, is varied from 25 to 600 μF. The energy, E, deposited by each discharger, D_1 or D_1, is calculated based on the capacitance, C, and voltage, U; that is, $E = E_p + CU^2/2$. After a discharge, the residual voltage of the capacitor does not exceed 400 V; i.e., the residual energy is less than 4% of the calculated energy E. The error in determining the voltage, $\Delta U/U$, is composed of several factors. The error in the threshold value U_T is determined by the threshold circuit and does not exceed 0.5% at the nominal voltage of 2000 V. It was found in the set of special tests that fluctuations in the network voltage and interferences of all kinds resulted in the uncertainty in the threshold value U_T not exceeding 0.5% at the nominal voltage of 2000 V. Therefore the total error in determining the capacitor voltage is estimated as less than 1%. The uncertainty in the C value is less than 1% too. Thus, the uncertainty in determining the energy E, calculated as $\Delta E/E = \Delta C/C + 2\Delta U/U$, does not exceed 3% at a voltage of 2000 V. Taking into account the residual energy in the capacitors, the maximal error in determining the E value based on the formula given above does not exceed 7%.

The electric scheme of the discharge timing diagnostics utilizes a single control channel to detect two synchronizing signals, S_1 and S_2, and two signals of the discharge currents J_1 and J_2 for determining the actual delay times $\Delta\tau_1$, $\Delta\tau_2$, and Δt_d. The discharge currents were measured by means of the Rogovsky coils.

D. Air-Assist Atomizer

Figure 4 shows the schematic of the air-assist atomizer used. The air is supplied via six radial channels 2.6 mm in diameter and 7 mm long. The liquid fuel is supplied via two fine axial channels 0.26 mm in diameter and 1 mm long normal to the air channels. The diameter of the atomizer nozzle is 6 mm. The air manifold is a flexible tube 28 mm in diameter and 800 mm long. The fuel manifold is a stainless steel tube 4 mm in diameter and 500 mm long.

To measure the drop size distribution the slide sampling method[27] was used. In this method, a slide with thinly coated soot deposited from a candle flame is introduced into the fuel spray for a short time. The footprints left by the impinging droplets in the soot are then photographed under the microscope. Figure 5 shows a photograph of the spray signature on a slide plate at a position close to the electrodes of the discharger D_1: 70 mm downstream from the atomizer nozzle. (White dots correspond to footprints left by impinging droplets.) At

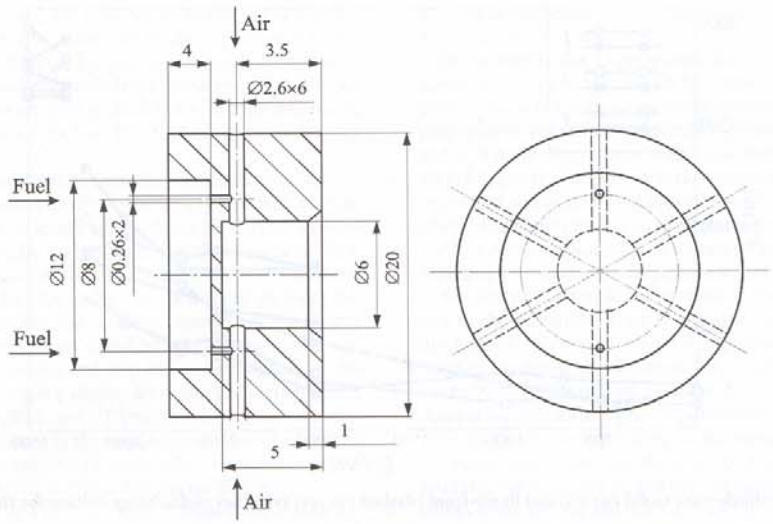

Fig. 4 Schematic of the air-assist atomizer. Dimensions in millimeters.

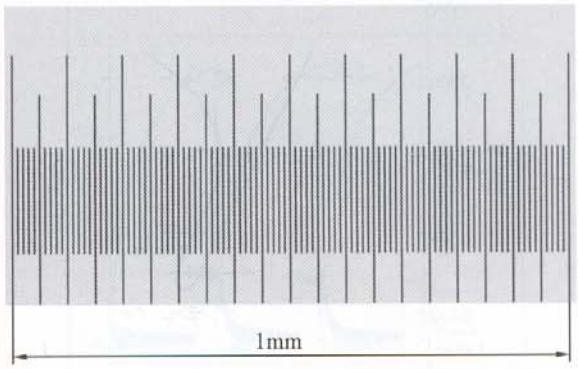

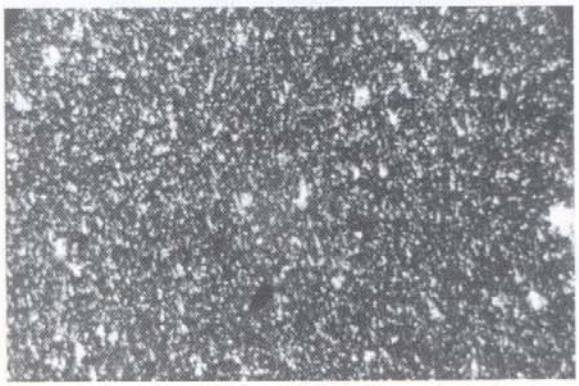

Fig. 5 Photograph of the *n*-hexane spray signature on the slide plate.

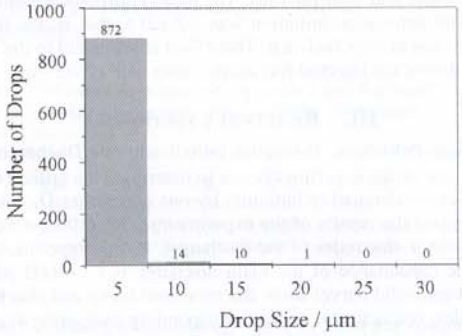

Fig. 6 Measured drop size distribution in an *n*-hexane spray.

distances exceeding 300 mm, no drops were detected in the flow, due to their virtually complete evaporation caused by the high volatility of *n*-hexane. Figure 6 shows the drop size distribution obtained from Fig. 5. The arithmetic mean diameter of the drops produced by the atomizer is close to 5 μm. In view of the data presented in Figs. 5 and 6, the discharger D_1 is located in the two-phase flow region during the experiments. As the discharger D_2 is positioned 200 mm downstream from the discharger D_1, it is still located in a two-phase flow region. Note that the measurements without ignition reveal the existence of a liquid fuel film deposited on the inner tube wall up to the distances of about 600 mm from the atomizer nozzle. In the experiments, the ignition occurs while the fuel is still supplied to the atomizer. Therefore the fuel prevaporization degree at the location of the discharger D_1 is nearly zero. As for the fuel prevaporization degree at the location of the discharger D_2, it can attain 95%. This percentage was estimated based on the knowledge of the mean initial drop size (5 μm), the measured spray penetration length (300 mm), and the mean airflow velocity. The measurements of the airflow velocity generated by the atomizer were made using the Pitot technique.[17,18] The measurements indicate that 260 mm downstream from the atomizer nozzle (at the position of the discharger D_2) the mean flow velocity is nearly constant across the tube and equal to (10 ± 1) m/s.

The air bottle and fuel tank were pressurized to the preset pressure values before each run, usually 6.00 ± 0.05 and 5.3 ± 0.05 atm, respectively. These values were found in a series of experiments aimed at establishing the optimal fuel-supply pressure at a given air pressure.[17,18] The optimal pressure provided the maximum visible flame propagation velocity in the setup of Fig. 1 when other conditions were fixed. The initial temperature of air and liquid fuel was 293 ± 4 K. In the course of the experiments, the tube temperature varied from 293 ± 4 K at the beginning of the run and did not exceed 310 K at the end of the run. The atomizer provided a flow rate of air of about 30 g/s. During an experimental run, the air pressure in the bottle did not drop below 4.8 atm.

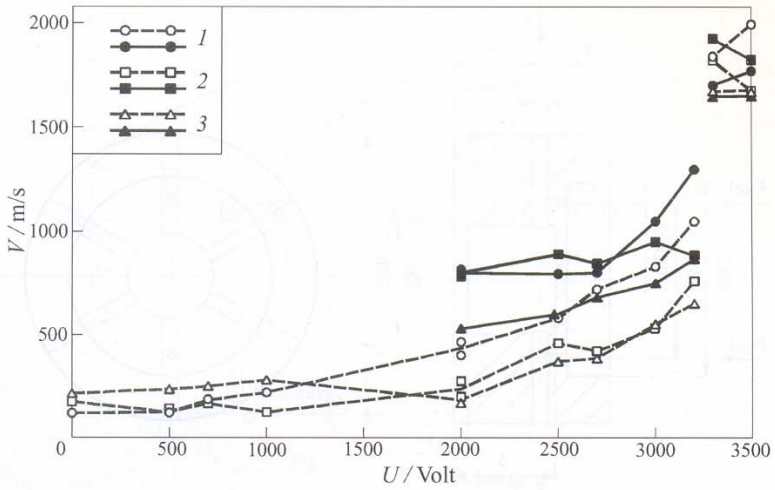

Fig. 7 Measured mean shock-wave (solid curves) and flame-front (dashed curves) velocities vs discharge voltage for the *n*-hexane–air mixture.

The fuel consumption was measured by the weighting technique in several experimental runs at similar initial conditions. Air consumption was calculated based on the pressure difference in the air bottle before and after the runs. The mean equivalence ratio in the runs with detonation initiation was 1.3 ± 0.1; that is, the fuel–air mixture was always fuel-rich. This effect is attributed to the partial deposition of the injected fuel on the inner wall of the tube.

III. Results of Experiments

A. Single-Pulse Spray Detonation Initiation by One Discharger

The aim of the experiments was to determine the critical energy E_{cr} of direct detonation initiation by one discharger D_1. Figure 7 summarizes the results of the experiments with different voltages at the power electrodes of the discharger. In this experimental series, the capacitance of the main discharge is $C_1 = 600$ μF. The dashed and solid curves show the measured flame and shock wave velocities, respectively, at the corresponding measuring segments (denoted by numbers 1, 2, and 3). Because of poor accuracy of pressure measurements at low ignition energies, the measurements of the shock wave velocity were performed beginning from a voltage of 2000 V. It follows from Fig. 7 that the increase in the main discharge voltage from 0 to 2000 V shows almost no effect on the flame propagation velocity at measuring segments 2 and 3. Contrary to the flame behavior at these measuring segments, the flame velocity at the segment 1 increases gradually with the voltage. Finally, at voltages exceeding 3300 V, a detonation wave arises at all measuring segments from 1 to 3. By other words, at discharge energy E exceeding approximately 3.3 kJ, the direct initiation of a detonation in the *n*-hexane spray has been obtained. This value will be referred to as the critical energy, $E_{cr} = 3.3$ kJ, for the direct detonation initiation in the setup of Fig. 1 with one discharger D_1. Further increase of the discharge energy from 3.3 to 3.7 kJ exerted no effect on the detonation parameters. The arising detonation waves propagated at a constant mean velocity of 1780 ± 100 m/s at measuring segments 2 and 3.

B. Single-Pulse Spray Detonation Initiation by Two Dischargers

Single-pulse tests with two successively triggered dischargers positioned at a distance of 200 mm from each other resulted in the important finding demonstrated by Fig. 8. (Plus = go, minus = no go for detonation.) Here, the capacitance of the main discharge in both dischargers D_1 and D_2 is $C_1 = C_2 = 300$ μF; that is, the total capacitance is nearly the same as in the one-discharger experiments of Sec. III.A. Resonant conditions exist for the second discharger triggering in terms of the delay time, Δt_d. The lowest voltage required for detonation initiation with two successively triggered dischargers is 2500 V (with an optimal delay time of 270 μs) instead of 3300 V

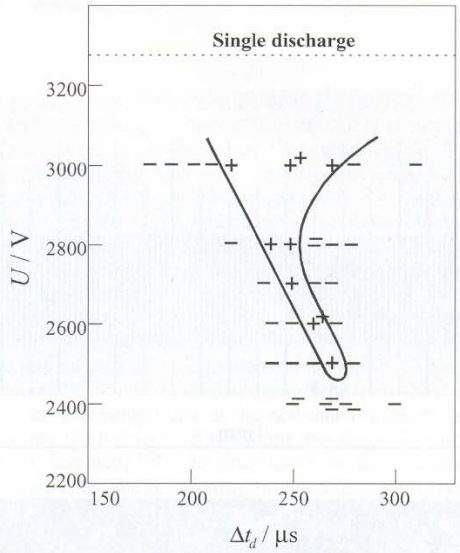

Fig. 8 Measured detonation initiation energy (in terms of the discharge voltage) as a function of the delay time Δt_d between triggering of two dischargers.

relevant to the case with one discharger. The curve in Fig. 8 will be referred to as the detonation peninsula. The "width" of the detonation peninsula is about 50 μs at 3000 V and 10 μs at 2500 V. At a fixed delay time, such as 270 μs, the detonation arises at 2500 V and does not arise at a higher voltage (2600 to 2900 V), which indicates the necessity of careful synchronization of the discharge triggering time with the arrival of the primary shock wave generated by the first discharger.

The decrease in the voltage from 3300 (the dotted line in Fig. 8) to 2500 V indicates an almost 43% (from 3.3 to 1.9 kJ) decrease in the total initiation energy and a 3.5-fold decrease in the energy deposited by each of the two dischargers (0.95 kJ) as compared to the energy of a single discharger (3.3 kJ) required for the direct detonation initiation.

C. Multipulse Spray Detonation Initiation by Two Dischargers

Figure 9 shows the registered time histories of the capacitor voltage U and air pressure in the air-assist atomizer for a series of three successive pulses in one experimental run. The supply of both air and fuel is activated when the capacitor voltage attains a preset value

equal to $0.95U_i$, where $U_i = 2700$ V is the discharge voltage in this experimental series. Similarly to Sec. III.B, the capacitance of the main discharge in the dischargers D_1 and D_2 is 300 μF. The voltage curves in Fig. 9 are reproduced well from pulse to pulse. The air pressure at the atomizer is set within about 0.1 s. During one pulse, the air pressure drops by 4% to 5%. The fuel pressure in the fuel unit is fixed at 5.3 atm.

Figure 10 shows a typical set of pressure records corresponding to all three successive pulses of Fig. 9 at nearly optimal detonation initiation conditions in terms of the delay time Δt_d between triggering the dischargers D_1 and D_2 (see Fig. 2) in each of three pulses and the fuel pressure in the air-assist atomizer. In addition to the pressure records, the diagnostics of each pulse includes the record of the control channel. The control channel record clearly shows the distortion of the ground signal by two synchronizing signals S_1 and S_2 (vertical spikes) and two successive signals of the dischargers D_1 and D_2 (sin wave shaped signals). The signals of the pressure transducers PT1, PT2, and PT3 are also distorted by the discharges nearly simultaneously. In the single-pulse mode, the optimal (required for detonation initiation) time delay between the discharges at $U = 2700$ V is $\Delta t_d = 250 \pm 10$ μs (see Fig. 8).

Based on the records of Fig. 10, Table 1 shows the actual delay times between two discharges, Δt_d, the measured values of the pressure wave arrival times at the transducers PT1, t_1, PT2, t_2, and PT3, t_3, and the estimated mean velocities of the pressure waves at the measuring segments 2 and 3, V_2 and V_3, in each pulse.

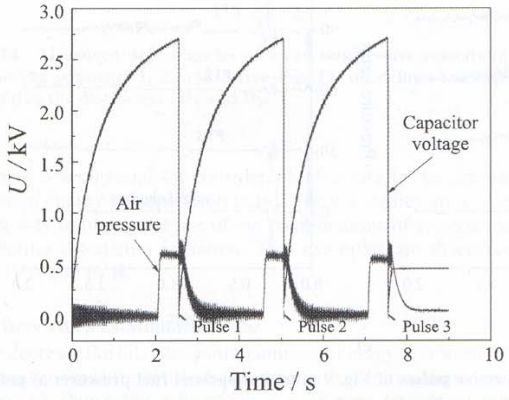

Fig. 9 Typical registered time histories of capacitor voltage, U, and the air pressure in the air-assist atomizer for the series of three successive pulses.

The mean velocities are estimated as $V_2 = 0.4/(t_2 - t_1)$ m/s and $V_3 = 0.2/(t_3 - t_2)$ m/s.

In the multipulse experiments, there is a slight variation in the actual delay time Δt_d caused by various destabilizing factors. At pulse 1, the accelerating explosion process is detected with the mean propagation velocity, V_3, increasing above 1400 m/s. At pulses 2 and 3, the pressure waves with detonation parameters ($V = 1700$–1800 m/s) form. The peak pressure (when noise is disregarded) in the registered waves attains values of 15–17 atm. The initiation energy of the detonation in this experiment with two dischargers is about 2.2 kJ per pulse. Note that detonation initiation in the experiments with a single discharger requires not less than 3.3 kJ per pulse.

Similarly to a single pulse, multipulse operation is very sensitive to the variation of the delay time Δt_d between triggering the dischargers. Figure 11 shows the pressure records obtained in a three-pulse run with the preset $\Delta t_d = 230$ μs, which is somewhat lower than the optimized value of $\Delta t_d = 250 \pm 10$ μs required for detonation initiation. Other experimental parameters were kept the same as those corresponding to the run of Fig. 10. Table 2 shows the actual delay time Δt_d, the measured values of the pressure wave arrival times t_1, t_2, and t_3, and the estimated velocities of the pressure waves at the second and third measuring segments V_2 and V_3 in each pulse. The detonation arises only at pulse 1, when the actual delay time Δt_d is accidentally optimal (apparently, due to the accidental distortion). When the delay time is 20 μs less than the optimal value, detonation initiation by two successively triggered dischargers fails, as was observed in the single-pulse runs too. At pulses 2 and 3, the decaying shock waves with propagation velocity $V = 600$–700 m/s are registered.

Table 1 Velocities at measuring segments 2 and 3 at nearly optimal delay time between triggering the dischargers

Pulse	Δt_d, μs	t_1, μs	t_2, μs	t_3, μs	V_2, m/s	V_3, m/s
1	260	709	1083	1224	1070 ± 8	1420 ± 26
2	270	562	794	904	1724 ± 20	1818 ± 40
3	250	550	778	886	1754 ± 20	1851 ± 40

Table 2 Velocities at measuring segments 2 and 3 at nonoptimal delay time between triggering the dischargers

Pulse	Δt_d, μs	t_1, μs	t_2, μs	t_3, μs	V_2, m/s	V_3, m/s
1	243	540	766	878	1770 ± 20	1785 ± 40
2	225	765	1315	1617	727 ± 4	662 ± 8
3	225	822	1438	1778	650 ± 4	588 ± 5

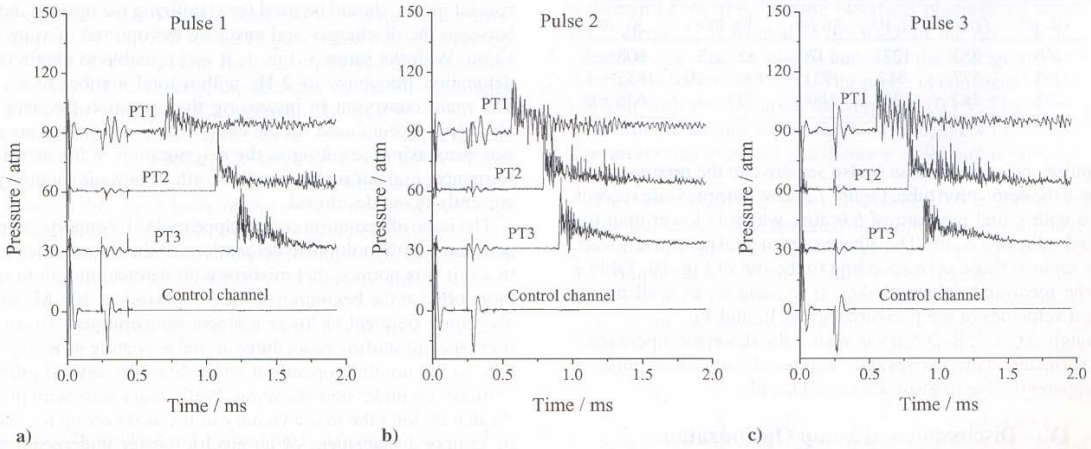

Fig. 10 Pressure records corresponding to the experimental run with three successive pulses of Fig. 9 and the record of the discharge control channel for the nearly optimal detonation initiation conditions: a) pulse 1, b) pulse 2, and c) pulse 3.

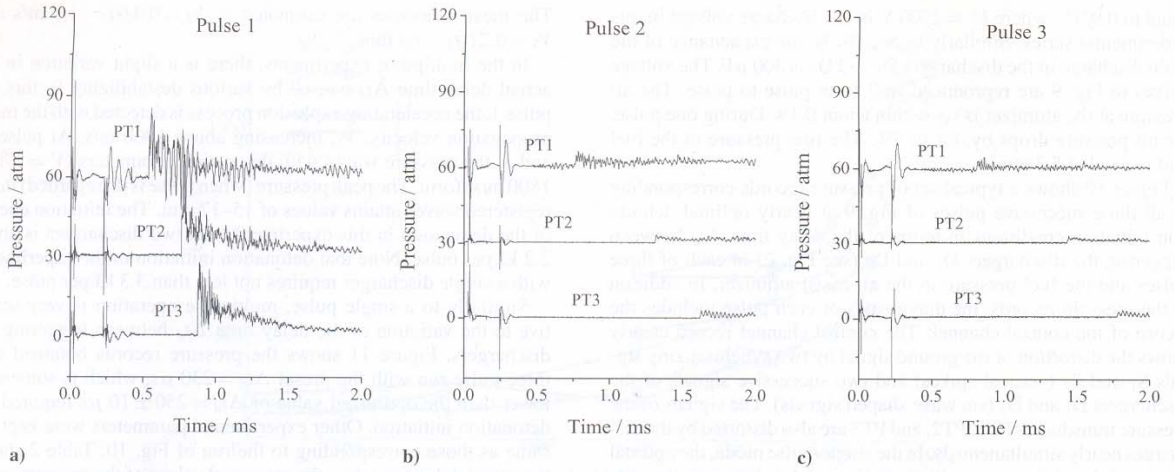

Fig. 11 Pressure records corresponding to the experimental run with three successive pulses of Fig. 9 at wrong discharge timing: a) pulse 1, b) pulse 2, and c) pulse 3.

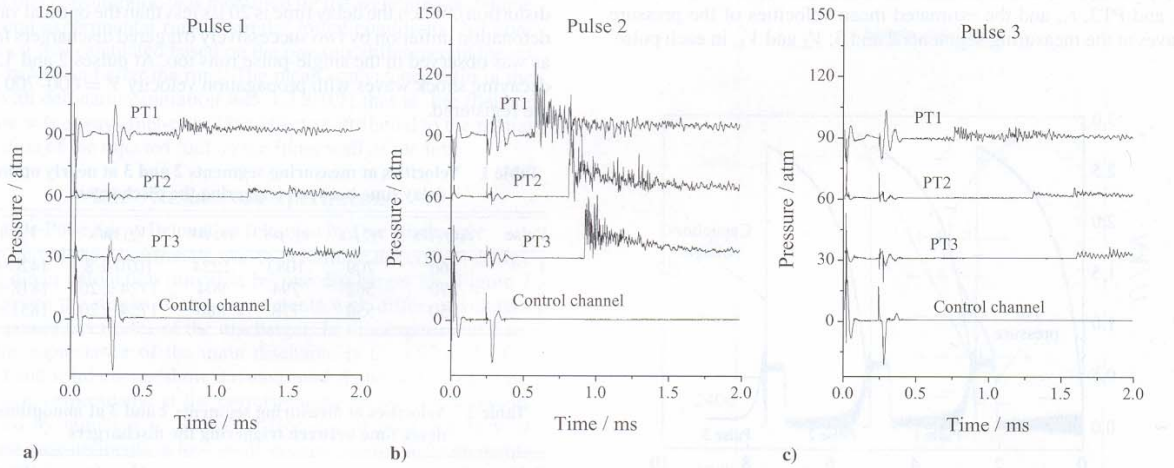

Fig. 12 Pressure records corresponding to the experimental run with three successive pulses of Fig. 9 at an nonoptimal fuel pressure: a) pulse 1, b) pulse 2, and c) pulse 3.

Table 3 Velocities at measuring segments 2 and 3 at nonoptimal pressure in the fuel supply line

Pulse	Δt_d, μs	t_1, μs	t_2, μs	t_3, μs	V_2, m/s	V_3, m/s
1	260	752	1221	1470	852 ± 5	803 ± 9
2	265	577	812	921	1702 ± 20	1835 ± 42
3	258	762	1304	1608	738 ± 4	658 ± 6

The pulse operation process is also sensitive to the mixture composition in the detonation tube. Figure 12 shows the pressure records obtained with a fuel pressure of 5.0 atm, which is lower than the optimized value of 5.3 atm. The other experimental parameters were kept the same as those corresponding to the run of Fig. 10. Table 3 shows the measured values of Δt_d, t_1, t_2, and t_3, as well as the estimated velocities of the pressure waves: V_2 and V_3.

Although $\Delta t_d = 258$–265 μs is within the detonation peninsula of Fig. 8, the detonation arises only at pulse 2 and fails at pulses 1 and 3, apparently due to insufficient fuel supply.

IV. Discussion and Setup Optimization

The experimental data indicate that both the single-pulse and multipulse operation modes exhibit resonant dependence of the detonation initiation energy on the time delay between discharge triggering and are quite sensitive to the mixture composition. Because of this, special means should be used for stabilizing the optimal delay time between the discharges and ensuring the optimal mixture composition. With the setup of Fig. 1, it was possible to obtain the pulse detonation frequency of 2 Hz with a total number of six pulses. The main constraint in increasing the operation frequency is the air supply system used. In the course of operation, the air pressure was decreasing, resulting in the deterioration of the atomizer performance, fuel–air mixing, and so forth. A new air supply system is currently being developed.

The issue of operation control appeared to be important. In the experiments with multipulse detonations of the liquid *n*-hexane spray in air, it was noticed that misfires with detonation failure occurred more often at the beginning of the run (as in Fig. 10). Misfires were also more frequent at lower ambient temperatures. To avoid misfires, special starting procedures aimed at heating up the detonation tube to the nominal operation temperature by several pulse deflagrations are under consideration. Preliminary tests with preheating the detonation tube in the vicinity of the atomizer up to 320–325 K by temporal placement of an electric heater underneath the tube avoided misfires completely. This is probably explained by faster vaporization of the fuel film deposited on the tube wall.

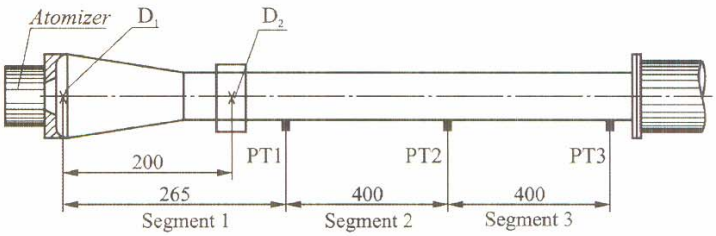

Fig. 13 Experimental setup with the 28-millimeter tube. Dimensions in millimeters.

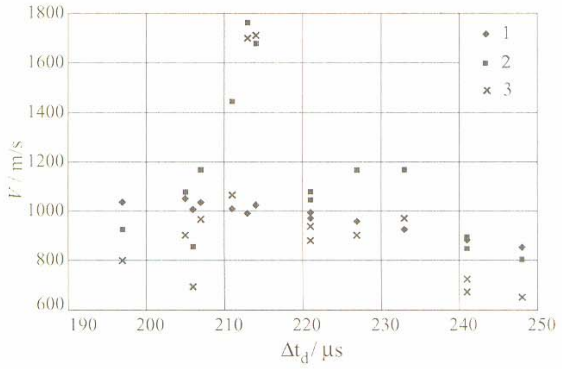

Fig. 14 Measured dependencies of mean shock wave velocity at the measuring segments 1, 2, and 3 (see Fig. 13) on delay time between triggering the dischargers D_1 and D_2.

There is a potential for considerable decrease in the detonation initiation energy per operation pulse. Special studies are currently under way implying the use of the combinations of various means promoting detonation initiation. Two examples are discussed in Sec. IV.A and IV.B.

A. Tests with a 28-Millimeter Tube

To decrease the total detonation initiation energy, it is worth while to operate with a tube of a diameter close to the limiting diameter.[17,18] Figure 13 shows the schematic of a 28-mm detonation tube—the smallest tube that allows the repeatable initiation of a liquid *n*-hexane spray–air detonation. In this setup, the first discharger is mounted close to the atomizer nozzle. The distance between the first and the second dischargers is 200 mm.

The tests on detonation initiation with one (first) discharger ($C_1 = 600\ \mu$F) have shown that the lowest voltage required for detonation initiation is $U = 1700$ V; that is, the critical initiation energy is about 0.92 kJ. The tests were made according to the procedure described in Sec. III.A. Clearly, the decrease in the tube diameter from 51 to 28 mm resulted in E_{cr} decreasing by a factor of 3.6.

The tests with two dischargers were made at capacitances $C_1 = C_2 = 200\ \mu$F and discharge voltage of $U = 2000$ V. Thus, the total energy provided by two dischargers was about 0.91 kJ. Figure 14 shows the dependence of the mean shock wave velocity on the triggering delay time Δt_d of the second discharger in the single-pulse mode. It is seen that the detonation was successfully initiated only within a very narrow range ("peninsula") of the triggering delay time: the detonation was detected at $211 < \Delta t_d < 221\ \mu$s. Figures 15a and 15b show the pressure records with successful detonation initiation ($\Delta t_d = 214\ \mu$s; Fig. 15a) and initiation failure ($\Delta t_d = 211\ \mu$s, Fig. 15b).

B. Tests with a 28-Millimeter Tube and Shchelkin Spiral

The air-assist atomizer provides a highly turbulent two-phase reactive flow in the detonation tube. The ignition of the flow with a powerful discharger results in the generation of a shock wave followed by the turbulent flame. The experimental results indicate (see, e.g., Fig. 7) that the propagation velocities of both the lead shock wave and the flame front are nearly independent of the discharge energy if the latter is less than about $0.35E_{cr}$. (The voltage is less than about 2000 V in Fig. 7.) This implies that at discharge energies less than $0.35E_{cr}$, the turbulence generated by the atomizer could determine the shock-wave and flame evolution. At higher discharge energies, the flame propagation is increasingly affected by the discharge-generated shock wave. In view of this, the enhancement of the turbulence produced by the atomizer could potentially be used for decreasing the discharge energy required for generating a powerful primary shock wave.

To check this implication, a special experimental study has been performed in the 28-mm diam tube with a turbulizing element in the form of a Shchelkin spiral. Figure 16 shows the schematic of the detonation tube with the Shchelkin spiral mounted between two dischargers, D_1 and D_2. The length of the spiral is 460 mm. It is made of steel wire 4 mm in diameter with a pitch of 18 mm and is installed in a tube section 500 mm long.

It is implied that the shock wave generated by the discharger D_1 and passed through the Shchelkin spiral can be further amplified to the detonation intensities by the properly tuned triggering of the discharger D_2 mounted downstream from the spiral section. The major energy is deposited by the discharger D_2. To provide the precise synchronization of the second discharger triggering with the shock wave arrival, a special discharge activation probe (see Fig. 16) was used. Attempts to implement a conventional pressure transducer for this purpose failed because of its sensitivity to noise. The pressure wave induced by the discharger D_1 had a relatively low amplitude, from 3 to 6 atm. Various disturbances caused by the electric discharge, interference, and pressure wave precursors propagating in the tube wall resulted in false operation of the system. The schematic of the probe and the corresponding electric circuit are shown in Fig. 17. It includes two parallel steel electrodes. The electrodes protrude from the tube wall normal to the axis. The electrode located upstream of the flow has the electrical potential of -300 V. The other electrode is located in the wake of the first one and is connected to the electric supply unit with the voltage of $+300$ V via a series resistor of 0.5 MΩ. The probe is connected to the threshold unit with the actuation threshold of 100 V. The probe triggers a time-delay circuit, which, in its turn, triggers the discharger D_2. The probe was mounted at a distance of 90 mm upstream from the discharger D_2.

The tests with one (first) discharger ($C_1 = 200\ \mu$F) and the Shchelkin spiral have revealed the following. At discharge energies considerably less than 0.1 kJ, the propagation velocities of the compression and combustion waves registered at the measuring segments 1–3 were close to the speed of sound in the initial mixture and shock waves did not form. Increasing the discharge energy to 0.1–0.13 kJ led to the formation of a shock wave with a propagation velocity of 910 ± 6 m/s at the measuring segment 2 and 770 ± 8 m/s at the measuring segment 3. At the measuring segment 1, the propagation velocities of the arising shock waves were close to the speed of sound. At higher discharge energies of 0.58–0.62 kJ, the situation changed: the shock wave velocity at measuring segment 1 was nearly independent of the discharge energy and equal

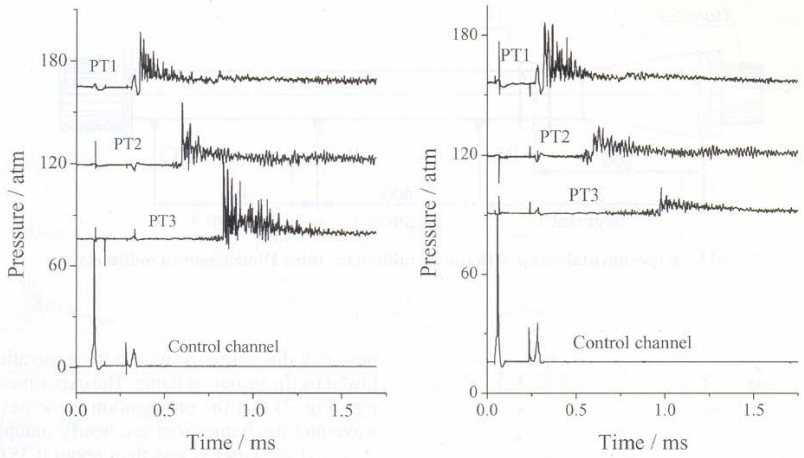

Fig. 15 Pressure records with a) successful detonation initiation (Δt_d = 214 μs) and b) initiation failure (Δt_d = 211 μs).

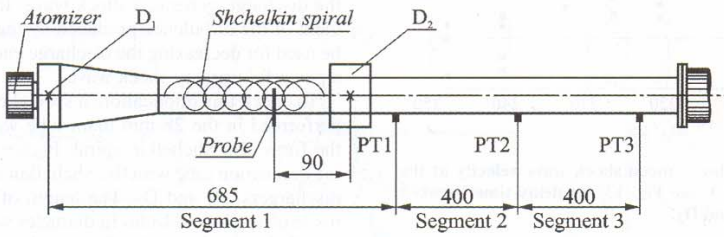

Fig. 16 Experimental setup with the 28-millimeter tube and the Shchelkin spiral between two dischargers. Dimensions in millimeters.

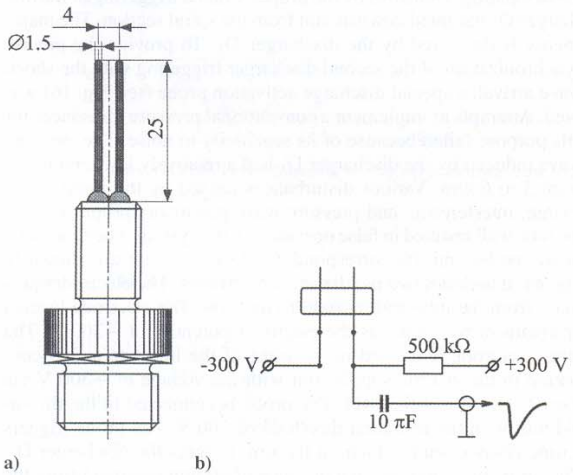

Fig. 17 Schematic of the discharge activation probe and the corresponding circuit.

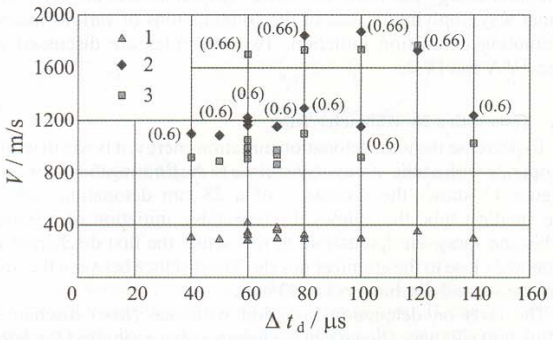

Fig. 18 Measured dependencies of the mean shock wave velocity on the delay time between the shock wave arrival at the probe and triggering of the second discharger.

to about 870 m/s, whereas at the measuring segments 2 and 3, the shock velocity decreased to 770–780 and 680–700 m/s, respectively. Clearly, the most efficient amplification of the shock waves in the spiral section was attained at the discharge energies of 0.1–0.13 kJ, from nearly the speed of sound to about 910 m/s. These values of the first discharge energy were treated as optimal for the tests with the Shchelkin spiral.

Further experiments were made to check the possibility to amplify the shock wave exiting from the Shchelkin spiral section by the properly tuned triggering of the discharger D_2. With the setup of Fig. 16, the total initiation energy required for the detonation initiation in the single-pulse mode was decreased to about 0.66 kJ. Table 4 summarizes the results of the experiments with the successful detonation initiation. Figure 18 shows the measured dependencies of the mean shock wave velocities on the delay time Δt_d between the shock-wave arrival at the probe and the triggering of the discharger D_2. At the total energy of two dischargers $E = 0.66$ kJ and at delay times of 60, 80, 100, and 120 μs, the detonation was registered at the measuring segments 2 and 3. Numbers in parentheses correspond to total initiation energy in kJ. Figure 19 shows the corresponding pressure records with successful detonation initiation. At $E = 0.605$ J and below, the detonation initiation failed. The delay time of 100 μs can be considered as the optimal value for the detonation initiation with two dischargers and the Shchelkin spiral. Note that $\Delta t_d = 100$ μs correlates with the time taken for the shock wave with the mean

Table 4 Results of experiments with successful detonation initiation in the 28-mm tube with two dischargers and the Shchelkin spiral

Run	t_1, μs	t_2, μs	t_3, μs	V_1, m/s	V_2, m/s	V_3, m/s	U, kV	C, μF	E, kJ	Δt_d, μs
1	1621	1855	2090	423 ± 5	1709 ± 20	1702 ± 38	2.2	275	0.665	60
2	2140	2357	2587	320 ± 4	1843 ± 23	1739 ± 40	2.3	250	0.661	80
3	2228	2441	2671	307 ± 4	1878 ± 23	1739 ± 40	2.3	250	0.661	100
4	1950	2177	2403	351 ± 5	1762 ± 22	1770 ± 40	2.3	250	0.661	120

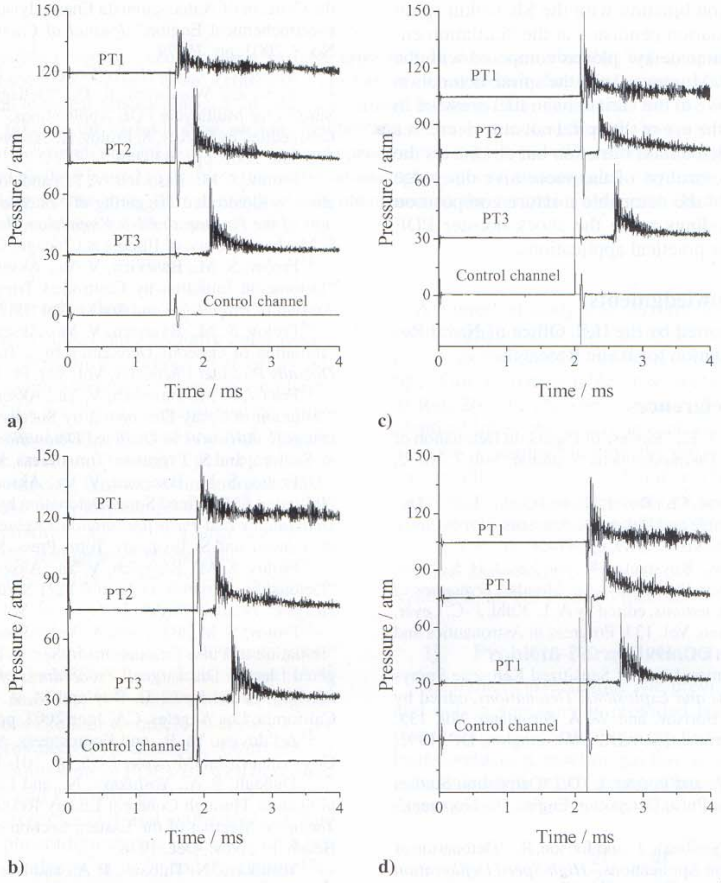

Fig. 19 Pressure records for four experimental runs with successful detonation initiation (see Table 4): a) run 1 with delay time Δt_d = 60 μs, b) run 2 with Δt_d = 80 μs, c) run 3 with Δt_d = 100 μs, and d) run 4 with Δt_d = 120 μs.

velocity of 910 m/s to travel a distance of 90 mm from the probe to the discharger.

Two very important findings follow from these experiments. First, it appears that the detonation peninsula in the tests with the Shchelkin spiral is considerably wider than in the tests without spiral. Recall that without spiral, the width of the detonation peninsula was about 10 μs (Fig. 14), whereas the spiral insert widens the peninsula to about 60 μs (Fig. 18). This is probably caused by the fact that the spiral modifies the pressure profile in the primary shock wave as compared with the cases without spiral. The pressure profile in a shock wave passed through the spiral becomes closer to a stepwise shape contrary to the triangular shape with fast pressure drop in a shock wave generated by the discharger D_1. Second, with the spiral, the dependencies $V(\Delta t_d)$ like those shown in Fig. 18 become less sensitive to the variations in fuel pressure in the air-assist atomizer. These findings indicate that the use of the Shchelkin spiral makes the shock-booster concept more feasible for practical applications.

Thus, it has been shown that the use of a 0.1–0.13-kJ discharge in combination with a relatively short Shchelkin spiral can result in the generation of a primary shock wave propagating at a velocity of about 910 m/s in a tube 28 mm in diameter. Such a shock wave can be amplified to a detonation by using an additional discharger triggered in phase with the shock wave arrival at its position.

The diameter of the tube used in the experiments of Sec. IV.A and IV.B is close to the limiting diameter. In such conditions, the detonations are marginally stable. As the experiments show, to initiate detonation by the successive triggering of several dischargers in such a tube, it is necessary to accelerate a shock wave to velocities exceeding 1400 m/s. In a larger tube 51 mm in diameter, this threshold velocity of a shock wave is about 1000 m/s. Clearly, the transition to the tubes of diameter somewhat larger than 28 mm will facilitate detonation initiation by the methods discussed herein.

V. Conclusions

Single-pulse and multipulse liquid *n*-hexane spray–air detonation initiation was demonstrated in short (about 1 m long) smooth-walled tubes 51 and 28 mm in diameter. Initiation schemes with a single electric discharger and two electric dischargers triggered successively were used. The minimal energy requirement for detonation

initiation in the 51-mm tube was found to be less than 1.9 kJ for the two-discharger scheme against 3.3 kJ for the one-discharger scheme. For the 28-mm tube, the minimal energy requirement for the two-discharger scheme was about 0.9 kJ, which was close to the critical initiation energy for one discharger (0.92 kJ). A possibility of further decreasing the total detonation initiation energy was successfully demonstrated in the single-pulse mode by using a combination of the two-discharger scheme with the Shchelkin spiral. The use of a spiral 460 mm long allowed the reduction of the total initiation energy to 0.66 kJ. It is shown that the use of two successively triggered dischargers in the combination with the Shchelkin spiral widens significantly the detonation peninsula at the "initiation energy vs discharge triggering time delay" plot as compared with the configuration without a spiral. Moreover, with the spiral, detonation initiation becomes less sensitive to the variations in fuel pressure in the air-assist atomizer. Thus, the use of the spiral not only decreases the energy requirements for detonation initiation but eliminates the necessity of accurate synchronization of the successive discharge triggering and maintenance of the detonable mixture composition in a narrow range. These findings make the shock-booster PDE concept[14–20] more feasible for practical applications.

Acknowledgments

This work was partly supported by the U.S. Office of Naval Research and the Russian Foundation for Basic Research.

References

[1]Borisov, A. A., and Gelfand, B. E., "Review of Papers on Detonation of Two-Phase Systems," *Archivum Thermodynamiki Spalania*, Vol. 7, No. 2, 1976, pp. 273–287.

[2]Samirant, M., Smeets, G., Baras, Ch., Royer, H., and Oudin, L. R., "Dynamic Measurements in Combustible and Detonable Aerosols," *Propellants, Explosives, Pyrotechnics*, Vol. 14, No. 1, 1989, pp. 47–56.

[3]Benedick, W. B., Tieszen, S. R., Knystautas, R., and Lee, J. H. S., "Detonation of Unconfined Large-Scale Fuel Spray–Air Clouds," *Dynamics of Detonations and Explosions: Detonations*, edited by A. L. Kuhl, J.-C. Leyer, A. A. Borisov, and W. A. Sirignano, Vol. 133, Progress in Astronautics and Aeronautics, AIAA, Washington, DC, 1991, pp. 297–310.

[4]Dabora, E. K., "Lean Detonation Limit of Sensitized Kerosene Sprays in Air," *Dynamics of Detonations and Explosions: Detonations*, edited by A. L. Kuhl, J.-C. Leyer, A. A. Borisov, and W. A. Sirignano, Vol. 133, Progress in Astronautics and Aeronautics, AIAA, Washington, DC, 1991, pp. 311–324.

[5]Brophy, C. M., Netzer, D. W., and Forster, L. D., "Detonation Studies of JP-10 with Air and Oxygen for Pulse Detonation Engine Development," AIAA Paper 98-4003, July 1998.

[6]Brophy, C. M., Netzer, D. W., Sinibaldi, J., and Jonson, R., "Detonation of JP-10 Aerosol for Pulse Detonation Applications," *High-Speed Deflagration and Detonation: Fundamentals and Control*, edited by G. Roy, S. Frolov, D. Netzer, and A. Borisov, Elex-KM, Moscow, 2001, pp. 207–222.

[7]Levin, V. A., Nechaev, J. N., and Tarasov, A. I., "A New Approach to Organize Operation Cycles in Pulsed Detonation Engines," *Journal of Chemical Physics Reports*, Vol. 20, No. 6, 2001, pp. 90–98 [in Russian]; also *High-Speed Deflagration and Detonation: Fundamentals and Control*, edited by G. Roy, S. Frolov, D. Netzer, and A. Borisov, Elex-KM, Moscow, 2001, pp. 223–238.

[8]Frolov, S. M., and Basevich, V. Ya., "Application of Fuel Blends for Active Detonation Control in a Pulsed Detonation Engine," ISABE Paper 99-135, Sept. 1999.

[9]Frolov, S. M., Basevich, V. Ya., and Vasil'ev, A. A., "Dual-Fuel Concept for Advanced Propulsion," *High-Speed Deflagration and Detonation: Fundamentals and Control*, edited by G. Roy, S. Frolov, D. Netzer, and A. Borisov, Elex-KM, Moscow, 2001, pp. 315–332.

[10]Knappe, B. M., and Edwards, C. F., "Investigation of Spray Detonation Characteristics Using a Controlled, Homogeneously Seeded Two-Phase Mixture," *Proceedings of the Fifteenth ONR Propulsion Meeting*, edited by G. D. Roy and A. K. Gupta, Univ. of Maryland, College Park, MD, Aug. 2002, pp. 172–177.

[11]Korobeinikov, V. P., Markov, V. V., Semenov, I. V., Pedrow, P. D., and Wojcicki, S., "Electrochemical Pulse Detonation Engine," *High-Speed Deflagration and Detonation: Fundamentals and Control*, edited by G. Roy, S. Frolov, D. Netzer, and A. Borisov, Elex-KM, Moscow, 2001, pp. 289–302.

[12]Korobeinikov, V. P., Markov, V. V., Semenov, I. V., and Wojcicki, S., "On the Concept of Autocyclomata Energodynamics and Modeling of the Pulse Electrochemical Engine," *Journal of Chemical Physics Reports*, Vol. 22, No. 8, 2003, pp. 75–79.

[13]Santoro, R. J., Lee, S.-Y., Conrad, C., Brumberg, J., Saretto, S., Lecat, P., Pal, S., and Woodward, R. D., "Deflagration-to-Detonation Transition Studies for Multicycle PDE Applications," *Advances in Confined Detonations*, edited by G. Roy, S. Frolov, R. Santoro, and S. Tsyganov, Torus Press, Moscow, 2002, pp. 243–249.

[14]Frolov, S. M., Basevich, V. Ya., and Aksenov, V. S., "Detonation Initiation by Controlled Triggering of Multiple Electric Discharges," *Proceedings of the Fourteenth ONR Propulsion Meeting*, edited by G. D. Roy and F. Mashayek, Univ. of Illinois at Chicago, Chicago, 2001, pp. 202–206.

[15]Frolov, S. M., Basevich, V. Ya., Aksenov, V. S., and Polikhov, S. A., "Detonation Initiation by Controlled Triggering of Electric Discharges," *Journal of Propulsion and Power*, Vol. 19, No. 4, 2003, pp. 573–580.

[16]Frolov, S. M., Basevich, V. Ya., Aksenov, V. S., and Polikhov, S. A., "Initiation of Gaseous Detonation by a Traveling Forced Ignition Pulse," *Doklady Physical Chemistry*, Vol. 394, Pt. 1, 2004, pp. 16–18.

[17]Frolov, S. M., Basevich, V. Ya., Aksenov, V. S., and Polikhov, S. A., "Initiation of Spray Detonation by Successive Triggering of Electric Discharges," *Advances in Confined Detonations*, edited by G. Roy, S. Frolov, R. Santoro, and S. Tsyganov, Torus Press, Moscow, 2002, pp. 150–157.

[18]Frolov, S. M., Basevich, V. Ya., Aksenov, V. S., and Polikhov, S. A., "Initiation of Confined Spray Detonation by Electric Discharges," *Confined Detonations and Pulse Detonation Engines*, edited by G. Roy, S. Frolov, R. Santoro, and S. Tsyganov, Torus Press, Moscow, 2003, pp. 157–174.

[19]Frolov, S. M., Basevich, V. Ya., Aksenov, V. S., and Polikhov, S. A., "Detonation Initiation in Liquid Fuel Sprays by Successive Electric Discharges," *Doklady Physical Chemistry*, Vol. 394, Pt. 2, 2004, pp. 39–41.

[20]Frolov, S. M., Basevich, V. Ya., Aksenov, V. S., and Polikhov, S. A., "Initiation of Pulse Detonations in Sprays by Means of Successively Triggered Electric Discharges," *Proceedings of the Sixteenth ONR Propulsion Meeting*, edited by G. D. Roy and M. A. Gundersen, Univ. of Southern California, Los Angeles, CA, June 2003, pp. 162–167.

[21]Zel'dovich, Ya. B., and Kompaneetz, A. S., *The Theory of Detonation*, Gostekhteorizdat, Moscow, 1955, pp. 101–112.

[22]Thibault, P. A., Yoshikava, N., and Lee, J. H. S., "Shock Wave Amplification Through Coherent Energy Release," Presented at the 1978 Fall Technical Meeting of the Eastern Section of the Combustion Inst., Miami Beach, FL, Nov.–Dec. 1978.

[23]Yoshikava, N, Thibault, P. A., and Lee, J. H. S., "Shock Wave Amplification in Non-Uniformly Preconditioned Gas Mixtures," Presented at the 1979 Spring Technical Meeting of the Canadian Section of the Combustion Inst., May 1979.

[24]Lee, J. H. S., Knystautas, R., and Yoshikawa, N., "Photochemical Initiation of Gaseous Detonations," *Acta Astronautica*, Vol. 5, No. 6, 1978, pp. 971–982.

[25]Lee, J. H. S., and Moen, I. O., "The Mechanism of Transition from Deflagration to Detonation in Vapor Cloud Explosions," *Progress in Energy and Combustion Sciences*, Vol. 6, No. 4, 1980, pp. 359–389.

[26]Roy, G. D., Frolov, S. M., Borisov, A. A., and Netzer, D. W., "Pulse Detonation Propulsion: Challenges, Current Status, and Future Perspective," *Progress in Energy and Combustion Sciences* (to be published).

[27]Elkotb, M. M., "Fuel Atomization for Spray Modelling," *Progress in Energy and Combustion Sciences*, Vol. 8, No. 1, 1982, pp. 61–91.